Narrow $J^\pi = 1/2^+, 3/2^+$, and $3/2^-$ states of Θ^+ in a quark model with antisymmetrized molecular dynamics

Y. Kanada-En'yo, O. Morimatsu, and T. Nishikawa
Institute of Particle and Nuclear Studies, High Energy Accelerator Research Organization, 1-1 Oho, Tsukuba, Ibaraki 305-0801, Japan
(Received 23 November 2004; published 6 April 2005)

The exotic baryon $\Theta^+(uudd\bar{s})$ is studied with microscopic calculations in a quark model by using a method of antisymmetrized molecular dynamics. We predict that three narrow states, $J^\pi = 1/2^+(I = 0)$, $J^\pi = 3/2^+(I = 0)$, and $J^\pi = 3/2^-(I = 1)$ nearly degenerate with the lowest $1/2^-$ state in the $uudd\bar{s}$ system. We discuss KN decay widths and estimate them to be $\Gamma < 7$ for the $J^\pi = \{1/2^+, 3/2^+\}$, and $\Gamma < 1$ MeV for the $J^\pi = 3/2^-$ state. In contrast to these narrow states, the $1/2^-$ states should be much broader. We assign the observed Θ^+ as the $J^\pi = \{1/2^+, 3/2^+\}$.

DOI: 10.1103/PhysRevC.71.045202 PACS number(s): 14.20.−c, 12.38.Aw, 12.39.Jh

I. INTRODUCTION

The exotic baryon Θ^+ has recently been reported by several experimental groups [1–9]. Because the quantum numbers determined from its decay modes indicate that the minimal quark content is $uudd\bar{s}$, these induced experimental and theoretical studies of multiquark hadrons. However, it should be kept in mind that the Θ^+ has not been well established yet because of the low statistics, and there is no evidence of the Θ^+ in some experiments [10–12].

The prediction of a $J^\pi = 1/2^+$ state of $uudd\bar{s}$ by a chiral soliton model [13] motivated the experiments of the first observation of Θ^+ [1]. Their prediction of even parity is unnatural in the naive quark model, because the lowest $q^4\bar{q}$ state is expected to be spatially symmetric and have odd parity because of the odd intrinsic parity of the antiquark. Theoretical studies were done to describe Θ^+ by many groups [14–21], some of which predicted the opposite parity, $J^\pi = 1/2^-$ [18–20]. The problem of spin and parity of Θ^+ is not only open but also essential to understand the dynamics of pentaquark systems. To solve this problem, it is crucial to calculate a five-quark system relying on fewer *a priori* assumptions such as the existence of quark clusters or the spin parity.

In this article we would like to clarify the mechanism of the existence of the pentaquark baryon and predict possible narrow Θ^+ states. We try to extract a simple picture for the pentaquark baryon with its energy, width, spin, parity and also its shape from explicit five-body calculation. To achieve this goal, we study the pentaquark with a flux-tube model [24,25] based on strong coupling quantum chromodynamics (QCD), by using a method of antisymmetrized molecular dynamics (AMD) [22,23]. In the flux-tube model, the interaction energy of quarks and antiquarks is given by the energy of the stringlike color-electric flux, which is proportional to the minimal length of the flux-tube connecting quarks and antiquarks at long distances supplemented by perturbative one-gluon-exchange (OGE) interaction at short distances. For the $q^4\bar{q}$ system the flux-tube configuration has an exotic topology [Fig. 1(c)], in addition to an ordinary meson-baryon topology [Fig. 1(d)], and the transition between different topologies takes place only in higher orders of the strong coupling expansion. Therefore, it seems quite natural that the flux-tube model accommodates the pentaquark baryon. In 1991, Carlson and Pandharipande studied exotic hadrons in the flux-tube model [26]. They calculated for only a few $q^4\bar{q}$ states with very limited quantum numbers and concluded that pentaquark baryons are absent. We apply the AMD method to the flux-tube model. The AMD is a variational method to solve a finite many-fermion system. This method is powerful for the study of nuclear structure. One of the advantages of this method is that the spatial and spin degrees of freedom for all particles are independently treated. This method can successfully describe various types of structure such as shell-model-like structure and clustering (correlated nucleons) in nuclear physics. In the application of this method to a quark model, we take the dominant terms of OGE potential and string potential because of the gluon flux tube. Different flux-tube configurations are assumed to be decoupled. Because we are interested in the narrow states, we only adopt the confined configuration given by Fig. 1(c). We calculate all the possible spin parity states of $uudd\bar{s}$ system and predict low-lying states. By analyzing the wave function, we discuss the properties of Θ^+ and estimate the decay widths of these states with a method of reduced width amplitudes.

This article is organized as follows. We explain the formulation of the present framework in the next section and show the results in Sec. III. In Sec. IV, we discuss the structure of low-lying states and their widths. Finally, we give a summary in Sec. V.

II. FORMULATION

In the present calculation, the quarks are treated as nonrelativistic spin-$\frac{1}{2}$ fermions. We use a Hamiltonian as follows:

$$H = H_0 + H_I + H_f, \tag{1}$$

where H_0 is the kinetic energy of the quarks, H_I represents the short-range OGE interaction between the quarks, and H_f is the energy of the flux tubes. For simplicity, we take into account the mass difference between the ud quarks and the s quark, only in the mass term of H_0 but not in the kinetic

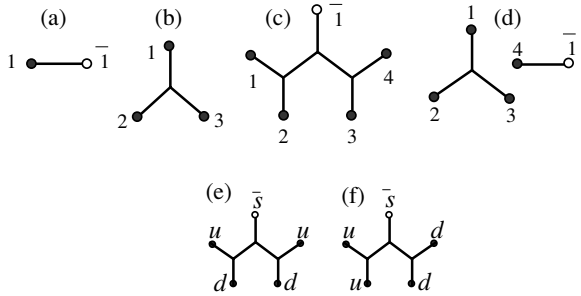

FIG. 1. Flux-tube configurations for confined states of $q\bar{q}$ (a), q^3 (b), $q^4\bar{q}$ (c) and the disconnected flux tube of $q^4\bar{q}$ (d). Figures (e) and (f) represent the flux tubes in the color configurations, $[ud][ud]\bar{s}$ and $[uu][dd]\bar{s}$, respectively.

energy term. Then, H_0 is represented as follows:

$$H_0 = \sum_i^{N_q} m_i + \sum_i^{N_q} \frac{p_i^2}{2m_q} - T_0, \tag{2}$$

where N_q is the total number of quarks and m_i is the mass of i-th quark, which is m_q for a u or d quark and m_s for a $\bar{s}$ quark. T_0 denotes the kinetic energy of the center-of-mass motion.

H_I represents the short-range OGE interaction between quarks and consists of the Coulomb and the color-magnetic terms as follows:

$$H_I = \alpha_c \sum_{i<j} F_i F_j \left[\frac{1}{r_{ij}} - \frac{2\pi}{3m_i m_j} s(r_{ij}) \sigma_i \cdot \sigma_j \right]. \tag{3}$$

Here, α_c is the quark-gluon coupling constant, and $F_i F_j$ is defined by $\sum_{\alpha=1,\ldots,8} F_i^\alpha F_j^\alpha$, where F_i^α is the generator of color SU(3), $\frac{1}{2}\lambda_i^\alpha$ for quarks and $-\frac{1}{2}(\lambda_i^\alpha)^*$ for antiquarks. The usual $\delta(r_{ij})$ function in the spin-spin interaction is replaced by a finite-range Gaussian, $s(r_{ij}) = [\frac{1}{2\sqrt{\pi}\Lambda}]^3 \exp[-\frac{r_{ij}^2}{4\Lambda^2}]$, as in Ref. [26]. Of course, the full OGE interaction contains other terms such as tensor and spin-orbit interactions. However, because our main interest here is to see the basic properties of the pentaquark, we do not include these minor contributions.

In the flux-tube quark model [24], the confining string potential is written as $H_f = \sigma L_f - M^0$, where σ is the string tension, L_f is the minimum length of the flux tubes, and M^0 is the zero-point string energy. M^0 depends on the topology of the flux tubes and is necessary to fit the $q\bar{q}$, q^3, and $q^4\bar{q}$ potential obtained from lattice QCD or phenomenology. In the present calculation, we adjust the M^0 to fit the absolute masses for each of three-quark and pentaquark.

For the meson and $3q$-baryon systems, the flux-tube configurations are the linear line and the Y-type configuration with three bonds and one junction as shown in Figs. 2(a) and 2(b), respectively. The string potential given by the Y-type flux tube in a $3q$-baryon system is supported by lattice QCD [27]. For the pentaquark system, the different types of flux-tube configurations appear as shown in Figs. 1(e), 1(f), and 1(d), which correspond to the states, $|\Phi_{(e)}\rangle = |[ud][ud]\bar{s}\rangle$, $|\Phi_{(f)}\rangle = |[uu][dd]\bar{s}\rangle$, and $|\Phi_{(d)}\rangle = |(qqq)_1(qq)_1\rangle$, respectively. ($[qq]$ is defined by color antitriplet of qq.) The flux-tube configuration shown in Figs. 1(e) and 1(f) have seven bonds and three

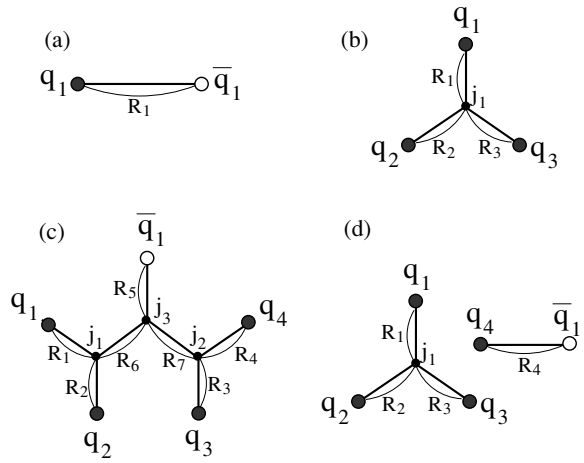

FIG. 2. Flux-tube topologies for the $q\bar{q}$ (a), q^3 (b), $[q_1q_2][q_3q_4]\bar{q}_1$ (c) and disconnected flux tubes (d) for the $(qqq)_1(q\bar{q})_1$. The flux-tube topologies are described by the bonds with the lengths R_k and the junctions j_k.

junctions, whereas the configuration in Fig. 1(d) has four bonds and one junction. In principle, in addition to these color configurations ($[qq][qq]\bar{q}$ and $(qqq)_1(qq)_1$), other color configurations are possible in totally color-singlet $q^4\bar{q}$ systems by incorporating a color-symmetric $(qq)_6$ pair as in Refs. [16,21]. However, because such a string from the $(qq)_6$ is energetically excited and is unfavored in the strong coupling limit of gauge theories as shown in Ref. [28], we consider only color-3 flux tubes as the elementary tubes. In fact, the string tension for the color-6 string in the strong coupling limit is $5/2$ times larger than that for the color-3 string from the expectation value of the Casimir operator. The string potentials given by the tube lengths of the configuration Fig. 1(c) is supported by lattice QCD calculations [29].

In the present calculation of the energy, we neglect the transition among $|\Phi_{(e)}\rangle$, $|\Phi_{(f)}\rangle$, and $|\Phi_{(d)}\rangle$ because they have different flux-tube configurations. It is reasonable in the first-order approximation, as mentioned. In each tube configuration, the minimum length L_f is given by a sum of the lengths (R_i) of bonds $L_f = R_1 + \cdots + R_k$ [k is the number of the bonds (see Fig. 2)]. Here we define L_{ij} to be the length of the path between i-th (anti-)quark and j-th (anti-)quark along the flux tubes. For example, in case of the $[qq][qq]\bar{q}$ state shown in Fig. 2(c), the path lengths are given by the bond lengths R_i as $L_{12} = R_1 + R_2$, $L_{13} = R_1 + R_6 + R_7 + R_3$, $L_{1\bar{1}} = R_1 + R_6 + R_5$, and so on. Then we can rewrite L_f in the expectation values of the string potential $\langle\Phi|H_f|\Phi\rangle$ with respect to a meson system($\Phi_{q\bar{q}}$), a three-quark system(Φ_{q^3}), and the pentaquark states $\Phi_{(e)}$, $\Phi_{(f)}$, $\Phi_{(d)}$, as follows:

$$L_f = L_{12} \quad \text{in } \langle\Phi_{q\bar{q}}|H_f|\Phi_{q\bar{q}}\rangle, \tag{4}$$

$$L_f = \tfrac{1}{2}(L_{12} + L_{23} + L_{31}) \quad \text{in } \langle\Phi_{q^3}|H_f|\Phi_{q^3}\rangle, \tag{5}$$

$$L_f = \tfrac{1}{2}(L_{12} + L_{34}) + \tfrac{1}{8}(L_{13} + L_{14} + L_{23} + L_{24}) + \tfrac{1}{4}(L_{\bar{1}1} + L_{\bar{1}2} + L_{\bar{1}3} + L_{\bar{1}4}) \quad \text{in } \langle\Phi_{(e,f)}|H_f|\Phi_{(e,f)}\rangle, \tag{6}$$

$$L_f = \tfrac{1}{2}(L_{12} + L_{23} + L_{31}) + L_{\bar{1}4} \quad \text{in } \langle\Phi_{(d)}|H_f|\Phi_{(d)}\rangle. \tag{7}$$

In the practical calculation, we approximate the minimum length of the flux tubes L_f by a linear combination of two-body distances r_{ij} between the i-th (anti-)quark and the j-th (anti-)quark as follows:

$$L_f \approx r_{12} \quad \text{in } \langle \Phi_{q\bar{q}}|H_f|\Phi_{q\bar{q}}\rangle, \tag{8}$$

$$L_f \approx \tfrac{1}{2}(r_{12}+r_{23}+r_{31}) \quad \text{in } \langle \Phi_{q^3}|H_f|\Phi_{q^3}\rangle, \tag{9}$$

$$L_f \approx \tfrac{1}{2}(r_{12}+r_{34}) + \tfrac{1}{8}(r_{13}+r_{14}+r_{23}+r_{24}) + \tfrac{1}{4}(r_{\bar{1}1}+r_{\bar{1}2}+r_{\bar{1}3}+r_{\bar{1}4}) \quad \text{in } \langle \Phi_{(e,f)}|H_f|\Phi_{(e,f)}\rangle, \tag{10}$$

$$L_f \approx \tfrac{1}{2}(r_{12}+r_{23}+r_{31}) + r_{\bar{1}4} \quad \text{in } \langle \Phi_{(d)}|H_f|\Phi_{(d)}\rangle. \tag{11}$$

It is clear that the above equations are obtained by approximating the path length L_{ij} with the distance r_{ij} as $L_{ij} \approx r_{ij}$ for all qq and $q\bar{q}$ pairs. In the meson system, Eq. (8) gives the exact L_f value. The approximation, Eq. (9), for $3q$ baryons is used in Ref. [24] and has been proved to be a good approximation. We note that the confinement is reasonably realized by the approximation in Eq. (10) for $\Phi_{(e,f)}$ as follows. The flux-tube configuration shown in Fig. 1(e) [and 1(f)] consists of seven bonds and three junctions. In the limit that the length (R_i) of any i-th bond becomes much larger than other bonds, the string potential $\langle H_f \rangle$ approximated by Eq. (10) behaves as a linear potential σR. It means that all the quarks and antiquarks are bound by the linear potential with the tension σ. In that sense, the approximation in Eq. (10) for the connected flux-tube configurations is regarded as a natural extension of the approximation [Eq. (9)] for $3q$ baryons. It is convenient to introduce an operator $\mathcal{O} \equiv -\frac{3}{4}\sigma \sum_{i<j} F_i F_j r_{ij} - M^0$. One can easily prove that the above approximations, Eqs. (8)–(11), are equivalent to $\langle\Phi|H_f|\Phi\rangle \approx \langle\Phi|\mathcal{O}|\Phi\rangle$ within each of the flux-tube configurations because the proper factors arise from $F_i F_j$ depending on the color configurations of the corresponding qq (or $q\bar{q}$) pairs.

To see the accuracy of the approximation Eqs. (9) and (10), we calculate the ratio of the approximated length $L_{\rm app}$ to the exact L_f in a simple quark distribution with Gaussian form that imitates the model wave function of the present calculation. Figure 3 shows the ratio $L_{\rm app}/L_f$ in a q^3 system and a $[qq][qq]\bar{q}$ system. The quark positions $\mathbf{r}_i$ are randomly chosen in Gaussian deviates with the probability $\rho = \exp(-r_i^2/b^2)$, and (L_f, $L_{\rm app}/L_f$) values for 1000 samplings are plotted. We use the same size parameter b as that of the single-particle Gaussian wave function in the present model explained later. Comparing Figs. 3(a) and 3(b), we found that the $L_{\rm app}/L_f$ ratio for the $[qq][qq]\bar{q}$ system is about 10% smaller than that for the q^3 system. Because the zero-point energy M_0 in the string potential is adjusted in each of the q^3 and the $[qq][qq]\bar{q}$, this underestimation should relate only to the relative energy of the string potential in each system and may give a minor effect on the level structure of the pentaquark.

We solve the eigenstates of the Hamiltonian with a variational method in the AMD model space [22,23]. We take a base AMD wave function in a quark model as follows:

$$\Phi(\mathbf{Z}) = (1 \pm P)\mathcal{A}\left[\phi_{\mathbf{Z}_1}\phi_{\mathbf{Z}_2}\cdots\phi_{\mathbf{Z}_{N_q}}X\right], \tag{12}$$

$$\phi_{\mathbf{Z}_i} = \left(\frac{1}{\pi b^2}\right)^{3/4} \exp\left[-\frac{1}{2b^2}(\mathbf{r}-\sqrt{2}b\mathbf{Z}_i)^2 + \frac{1}{2}\mathbf{Z}_i^2\right], \tag{13}$$

where $1 \pm P$ is the parity projection operator, $\mathcal{A}$ is the antisymmetrization operator, and the spatial part $\phi_{\mathbf{Z}_i}$ of the i-th single-particle wave function is given by a Gaussian whose center is located at $\mathbf{Z}_i$ in the phase space. X is the spin-isospin-color function. For example, in case of the proton, X is given as $X = (|\uparrow\downarrow\uparrow\rangle_S - |\uparrow\uparrow\downarrow\rangle_S) \otimes |uud\rangle \otimes \epsilon_{abc}|abc\rangle_C$. Here, $|m\rangle_S (m = \uparrow, \downarrow)$ is the intrinsic-spin function and $|a\rangle_C (a = 1, 2, 3)$ expresses the color function. Thus, the wave function of the N_q quark system is described by the complex variational parameters, $\mathbf{Z} = \{\mathbf{Z}_1, \mathbf{Z}_2, \ldots, \mathbf{Z}_{N_q}\}$. By using the frictional cooling method [22] the energy variation is performed with respect to $\mathbf{Z}$.

For the pentaquark system ($uudd\bar{s}$),

$$X = \sum_{m_1,m_2,m_3,m_4,m_5} c_{m_1m_2m_3m_4m_5}|m_1m_2m_3m_4m_5\rangle_S \otimes \{|udud\bar{s}\rangle \text{ or } |uudd\bar{s}\rangle\} \otimes \epsilon_{abg}\epsilon_{ceh}\epsilon_{ghf}|abce\bar{f}\rangle_C, \tag{14}$$

where $|udud\bar{s}\rangle$ and $|uudd\bar{s}\rangle$ correspond to the configurations $[ud][ud]\bar{s}$ and $[uu][dd]\bar{s}$ in Fig. 1, respectively. Because we are interested in the confined states, we do not use the meson-baryon states, $(qqq)_1(q\bar{q})_1$. This assumption of decoupling of the reducible and irreducible configurations of the flux tubes can be regarded as a kind of bound-state approximation. The decoupling of the different flux-tube configurations can be characterized by the suppression factor ϵ from the transition of the gluon field in the nondiagonal matrix elements $\epsilon\langle\Phi_1|\mathcal{O}|\Phi_2\rangle$. In a simple flux-tube model, ϵ is roughly estimated by the area Δ_s swept by the tubes when moving from one configuration into the other configuration as $\epsilon \sim \exp(-\sigma\Delta_s)$. We make an estimation of the expectation value of $\exp(-\sigma\Delta_s)$ by assuming a simple quark distribution with Gaussian form that imitates the model wave function in the same way as the evaluation of the $L_{\rm app}/L_f$. The

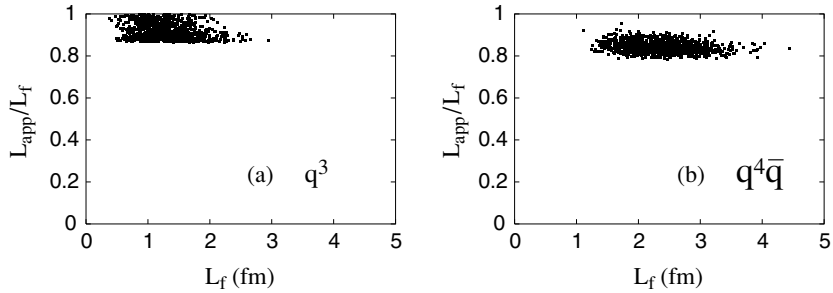

FIG. 3. The ratio $L_{\rm app}/L_f$ for the approximated tube length $L_{\rm app}$ and the exact tube length L_f in a q^3 system and a $[qq][qq]\bar{q}$ system. The quark positions $\mathbf{r}_i$ are randomly chosen in Gaussian deviates with the probability $\rho = \exp(-r_i^2/b^2)$, and (L_f, $L_{\rm app}/L_f$) values for 1000 samplings are plotted.

suppression factor ϵ among the configurations $[ud][ud]\bar{s}$, $[uu][dd]\bar{s}$, and $(qqq)_1(q\bar{q})_1$ is estimated to be $\epsilon^2 \lesssim 1/10$ within the present model space. Therefore, we consider that the present assumption of the complete decoupling $\epsilon = 0$ in the energy variation is acceptable in first-order calculations.

The coefficients $c_{m_1m_2m_3m_4m_5}$ for the spin function are determined by diagonalization of Hamiltonian and norm matrices. After the energy variation with respect to the $\{\mathbf{Z}\}$ and $c_{m_1m_2m_3m_4m_5}$, the intrinsic-spin and parity S^π eigenwave function $\Phi(\mathbf{Z})$ for the lowest state is obtained for each S^π. In the AMD wave function, the spatial wave function is given by multicenter Gaussians. When the Gaussian centers are located in some groups, the wave function describes the multicenter cluster structure and is equivalent to the Brink model wave function (a cluster model often used in nuclear structure study) [30,31]. Conversely, because of the antisymmetrization, it can also represent shell-model wave functions when all the Gaussian centers are located near the center of the system [30,31]. In nuclear structure study, it has been already proved that the AMD is one of the powerful tools because of the flexibility of the wave function [23]. In general, the relative motions in the AMD are given by such Gaussian forms as $\exp[-\nu'(\mathbf{x}-\mathbf{R})^2]$, where $\mathbf{x}$ is a Jacobi coordinate and $\mathbf{R}$ is given by a linear combination of the Gaussian centers $\{\mathbf{Z}_1, \mathbf{Z}_2, \ldots, \mathbf{Z}_{N_q}\}$. Here we explain the details of the relative motion in a simple case of a two-body cluster structure in a $N_q = 5$ system. If the Gaussian centers are located in two groups as $\mathbf{Z}_1 = \mathbf{Z}_2 = \mathbf{Z}_3 = \mathbf{Q}_1/\sqrt{2}b$ and $\mathbf{Z}_4 = \mathbf{Z}_5 = \mathbf{Q}_2/\sqrt{2}b$, and if each group contains no identical particles, the wave function expresses the two-body cluster state, where each cluster is the harmonic oscillator $0s$-orbital state, $(0s)^{2,3}$, with zero orbital-angular momentum. The intercluster motion $\mathcal{X}$ is given as $\mathcal{X}(\mathbf{x}, \mathbf{R}, \nu') = \exp[-\nu'(\mathbf{x}-\mathbf{R})^2]$, where $\nu' = \frac{3}{5b^2}$, $\mathbf{R} = \mathbf{Q}_2 - \mathbf{Q}_1$ and $\mathbf{x}$ is the relative coordinate between the clusters. In the partial wave expansion of the intercluster motion $\mathcal{X}$,

$$\begin{aligned}\mathcal{X}(\mathbf{x}, \mathbf{R}, \nu') &= \exp[-\nu'(\mathbf{x}-\mathbf{R})^2], \\ &= \Sigma_L 4\pi i_L(2\nu' Rx) e^{-\nu'(x^2+R^2)} \\ &\quad \times \Sigma_M Y_{LM}(\hat{x}) Y^*_{LM}(\hat{R}),\end{aligned} \tag{15}$$

where i^L is the modified spherical Bessel function, it is found that the wave function contains higher orbital-angular momentum L components in general. However, in the case of $\nu' R^2 \leqslant O(1)$, the wave function is dominated by the lowest L component because the L components rapidly decrease with the increase of L. As a result, the even-parity $S^{\pi=+}$ 3^q and odd-parity $q^4\bar{q}$ states are almost the $L = 0$ eigenstates, whereas the odd-parity 3^q and even-parity $q^4\bar{q}$ states are nearly the $L = 1$ eigenstates. (The $q^4\bar{q}$ contains an odd intrinsic parity of the $\bar{q}$ in addition to the parity of the spatial part.) Therefore, we do not perform the explicit L projection in present calculation for simplicity. We have actually checked that the obtained wave functions are almost the L eigenstates ($L = 0$ or 1) and higher L components are minor in most of the q^3 and $q^4\bar{q}$ states.

In the present wave function we do not explicitly perform the isospin projection; however, the wave functions obtained by energy variation are found to be approximately isospin-eigenstates in most of the low-lying states of the q^3 and $q^4\bar{q}$ because of the color-spin symmetry.

In the numerical calculation, the linear and Coulomb potentials are approximated by seven-range Gaussians. We use the following parameters:

$$\begin{aligned}\alpha_c &= 1.05, \\ \Lambda &= 0.13\,\text{fm}, \\ m_q &= 0.313\,\text{GeV}, \\ m_s &= 0.513\,\text{GeV}, \\ \sigma &= 0.853\,\text{GeV/fm}.\end{aligned} \tag{16}$$

Here, the quark-gluon coupling constant α_c is chosen to fit the N and Δ mass difference. The string tension σ is adopted to adjust the excitation energy of $N^*(1520)$. The size parameter b is chosen to be 0.5 fm.

III. RESULTS

In Table I, we display the calculated energy of q^3 states with $S^\pi = 1/2^+(N)$, $S^\pi = 3/2^+(\Delta)$, and $S^\pi = 1/2^-(N^*)$. The zero-point energy M^0 of the string potential is chosen to be $M^0_{q^3} = 972$ MeV to fit the masses of q^3 systems, N, N^*, and Δ. The calculated masses for Λ with $S^\pi = 1/2^-$ and $1/2^+$ correspond to the experimental data of $\Lambda(1115)$ and $\Lambda^*(1670)$. The contributions of the kinetic and each potential term are consistent with the results of Ref. [26]. We checked that the obtained states are almost eigenstates of the angular momentum L and the L projection gives only minor effects on the energy.

TABLE I. Calculated masses (GeV) of the q^3 systems. The expectation values of the kinetic, string, Coulomb, and color-magnetic terms are also listed.

S^π	$(uud)_1$ $\frac{1}{2}^+$	$(uud)_1$ $\frac{1}{2}^-$	$(uuu)_1$ $\frac{3}{2}^+$	$(uds)_1$ $\frac{1}{2}^+$	$(uds)_1$ $\frac{1}{2}^-$
Kinetic (H_0)	1.74	1.87	1.66	1.93	2.09
String (H_F)	0.02	0.27	0.07	0.03	0.25
Coulomb	−0.65	−0.52	−0.62	−0.65	−0.53
Color mag.	−0.17	−0.09	0.14	−0.16	−0.14
E	0.94	1.52	1.24	1.14	1.67
Exp. (MeV)	$N(939)$	$N^*(1520)$, $N^*(1535)$	$\Delta(1232)$	$\Lambda(1115)$	$\Lambda(1670)$

TABLE II. Calculated masses (GeV) of the $uudd\bar{s}$ system. $M^0_{q^4\bar{q}} = 2385$ MeV is used to adjust the energy of the lowest state to the observed mass. The expectation values of the kinetic, string, Coulomb, and color-magnetic terms and that of the color-magnetic term in $q\bar{q}$ pairs are listed. In addition to the lowest $1/2^-$ state with the $[uu][dd]\bar{s}$ configuration, we show the results of the $1/2^-$ state with $[ud][ud]\bar{s}$ configuration, which lies in the low-energy region.

S^π	$[uu][dd]\bar{s}$ $\frac{1}{2}^-$	$[ud][ud]\bar{s}$ $\frac{3}{2}^-$	$[ud][ud]\bar{s}$ $\frac{1}{2}^+$	$[ud][ud]\bar{s}$ $\frac{1}{2}^-$	$[uu][dd]\bar{s}$ $\frac{5}{2}^-$	$[ud][ud]\bar{s}$ $\frac{3}{2}^+$	$[ud][ud]\bar{s}$ $\frac{5}{2}^+$
Kinetic (H_0)	3.23	3.22	3.36	3.19	3.19	3.36	3.33
String (H_F)	−0.67	−0.66	−0.55	−0.64	−0.64	−0.56	−0.54
Coulomb	−1.05	−1.04	−0.99	−1.03	−1.03	−0.99	−0.98
Color mag.	−0.01	0.01	−0.25	0.04	0.19	−0.06	0.17
$q\bar{q}$Color mag.	−0.06	−0.01	0.00	0.02	0.06	0.02	0.04
E	1.50	1.53	1.56	1.56	1.71	1.75	1.98

Now, we apply the AMD method to the $uudd\bar{s}$ system. For each spin parity, we calculate energies of the $[ud][ud]\bar{s}$ and $[uu][dd]\bar{s}$ states and adopt the lower one. In Table II, the calculated results are shown. We adjust the zero-point energy of the string potential M_0 as $M^0_{q^4\bar{q}} = 2385$ MeV to fit the absolute mass of the recently observed Θ^+. This $M^0_{q^4\bar{q}}$ for pentaquark system is chosen independently of $M^0_{q^3}$ for $3q$ baryon. If $M^0_{q^4\bar{q}} = \frac{5}{3}M^0_{q^3}$ is assumed as in Ref. [26], the calculated mass of the pentaquark is around 2.2 GeV, which is consistent with the result of Ref. [26].

The most striking point in the results is that the $S^\pi = 3/2^-$ and $S^\pi = 1/2^+$ states nearly degenerate with the $S^\pi = 1/2^-$ states. The $S^\pi = 1/2^+$ correspond to $J^\pi = \{1/2^+, 3/2^+\}$ ($S = 1/2, L = 1$), and the $S^\pi = 3/2^-$ is $J^\pi = 3/2^-(S = 3/2, L = 0)$. The lowest $S^\pi = 1/2^-(J^\pi = 1/2^-, L = 0)$ state appears just below the $S^\pi = 3/2^-$ and the second $S^\pi = 1/2^-(J^\pi = 1/2^-, L = 0)$ state is at the same energy as the $S^\pi = 1/2^+(J^\pi = 1/2^+, 3/2^+, L = 1)$ states. However, these $J^\pi = 1/2^-$ states, as we discuss later, are expected to be much broader than other states. The $J^\pi = 1/2^+$ and $3/2^+$ exactly degenerate in the present Hamiltonian that does not contain the spin-orbit force. Other spin-parity states are much higher than these low-lying states.

IV. DISCUSSION

In this section, we analyze the structure of the obtained low-lying states of the $uudd\bar{s}$ system and discuss the level structure and the width for KN decays.

A. Structure of low-lying states

We analyzed the spin structure of these states and found that the $J^\pi = \{1/2^+, 3/2^+\}$ states consist of two spin-zero $[ud]$ pairs, whereas the $J^\pi = 3/2^-$ contains of a spin-zero $[ud]$ pair and a spin-one $[ud]$ pair. Here we call the color antitriplet qq pair with the same spatial single-particle wave functions a $[qq]$ pair and note a spin S $[qq]$ pair as $[qq]^S$. Because the $[ud]^0$ pair has the isospin $I = 0$ and the $[ud]^1$ pair has the isospin $I = 1$ because of the color asymmetry, the $J^\pi = 3/2^-$ state is isovector, whereas the lowest even-parity $J^\pi = \{1/2^+, 3/2^+\}$ states are isoscalar. The $J^\pi = 1/2^+$ state corresponds to the $\Theta^+(1530)$ in the flavor $\overline{10}$-plet predicted by Diakonov *et al.* [13]. It is surprising that the odd-parity state, $J^\pi = 3/2^-$ has the isospin $I = 1$, which means that this state is a member of the flavor 27-plet and belong to a new family of Θ baryon. We denote the $J^\pi = \{1/2^+, 3/2^+\}$, $I = 0$ states by Θ^+_0 and the $J^\pi = 3/2^-$, $I = 1$ state by Θ^+_1. The mass difference $E(\Theta^+_0) - E(\Theta^+_1)$ is about 30 MeV. In the energy region compatible to the $J^\pi = \{1/2^+, 3/2^+\}$ and $J^\pi = 3/2^-$ states, there appear two $J^\pi = \{1/2^-\}$ states. The lowest one is the $[uu][dd]\bar{s}$ state with $[uu]^1$ and $[dd]^1$ pairs, whereas the higher one is the $[ud][ud]\bar{s}$ with $[ud]^0$ and $[ud]^1$ pairs. The former is the isospin symmetric state and is dominated by $I = 0$ component. The latter is isovector and is regarded as the spin S partner of the $J^\pi = 3/2^-$ state. The $J^\pi = 1/2^-$ state is the lowest in the $uudd\bar{s}$ system. We, however, consider this state not to be the observed Θ^+ because its width should be broad as discussed later.

Although it is naively expected that unnatural spin parity states are much higher than the natural spin-parity $1/2^-$ state, the present results show the abnormal level structure of the $(udud\bar{s})$ system, where the high spin $J^\pi = 3/2^-$ state and the unnatural parity $J^\pi = \{1/2^+, 3/2^+\}$ states nearly degenerate just above the $J^\pi = 1/2^-$ state. By analyzing the details of these states, the abnormal level structure can be easily understood with a simple picture as follows. As shown in Table II, the $J^\pi = \{1/2^+, 3/2^+\}(L = 1)$ states have larger kinetic and string energies than the $J^\pi = 3/2^-(L = 0)$ and $J^\pi = 1/2^-(L = 0)$ states, whereas the former states gain the color-magnetic interaction. It indicates that the degeneracy of parity-odd states and parity-even states is realized by the balance of the loss of the kinetic and string energies and the gain of the color-magnetic interaction. In the $J^\pi = \{1/2^+, 3/2^+\}$ and the $J^\pi = 1/2^-, 3/2^-$ states, the competition of the energy loss and gain can be understood by Pauli principle from the point of view of the $[qq]$ pair structure as follows. As already mentioned by Jaffe and Wilczek [14], the relative motion between two $[qq]^0$ pairs must have the odd parity ($L = 1$) because the $L = 0$ is forbidden between the two identical $[qq]$ pairs because of the color antisymmetry. In the $J^\pi = 3/2^-$ state and the second $J^\pi = 1/2^-$ state, one of the $[ud]^0$ pairs is broken to be a $[ud]^1$ pair and the $L = 0$ is allowed because two diquarks are not identical. The $L = 0$

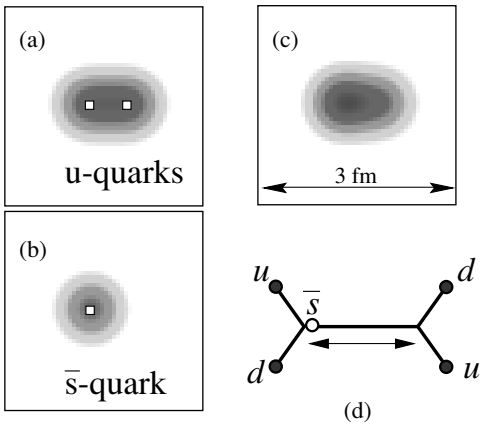

FIG. 4. The q and $\bar{q}$ density distribution in the $J^\pi = 1/2^+, 3/2^+ (S = 1/2, L = 1)$ states of the $uudd\bar{s}$ system. The u density (a), $\bar{s}$ density (b), and total quark-antiquark density (c) of the intrinsic state before parity projection are shown. The schematic figure of the corresponding flux-tube configuration is illustrated in (d). Open squares in (a) and (b) indicate the positions of Gaussian centers $\mathrm{Re}[\sqrt{2}b\mathbf{Z}_i]$ for the i-th single-particle wave functions.

is energetically favored in the kinetic and string terms, and the energy gain cancels the color-magnetic energy loss of a $[ud]^1$ pair. Also in the lowest $J^\pi = 1/2^-$ state, the competition of energy loss and gain is similar; each contribution of the kinetic, string, and potential energies in the lowest $J^\pi = 1/2^-$ state is almost the same as those in the $J^\pi = 3/2^-$ and the second $J^\pi = 1/2^-$(Table II). It means that the gain of the kinetic energy of the $L = 0$ state competes with the color-magnetic energy loss in the lowest $J^\pi = 1/2^-$ as well as the $J^\pi = 3/2^-$ and the second $J^\pi = 1/2^-$.

We should stress that the existence of two spin-zero ud diquarks in the $J^\pi = \{1/2^+, 3/2^+\}$ states predicted by Jaffe and Wilczek [14] is actually confirmed in the present calculations without *a priori* assumptions for the spin and spatial configurations. In fact, the component with two spin-zero $[ud]$ pairs is 97% in the present $J^\pi = \{1/2^+, 3/2^+\}$ state. In Fig. 4, we show the quark and antiquark density distribution in the $J^\pi = \{1/2^+, 3/2^+\}$ states and display the centers of Gaussians for the single-particle wave functions. In the intrinsic wave function, Gaussian centers for two $[ud]^0$ pairs are located far from each other with the distance about 0.6 fm. This indicates the spatially developed diquark-cluster structure, which means the spatial and spin correlations in each $[ud]$ pair. It is found that the center of the $\bar{s}$ stays at the same point of that of one $[ud]^0$, as $\mathbf{Z}_1 = \mathbf{Z}_2 = \frac{3}{5\sqrt{2}b}\mathbf{Q}_{12}$ and $\mathbf{Z}_3 = \mathbf{Z}_4 = \mathbf{Z}_5 = -\frac{2}{5\sqrt{2}b}\mathbf{Q}_{12}$, where $\{\mathbf{Z}_1, \mathbf{Z}_2, \ldots, \mathbf{Z}_5\}$ are the Gaussian centers in Eq. (12) and $|\mathbf{Q}_{12}| \sim 0.6$ fm. As a result, we found the spatial development of ud-uds clustering and a parity-asymmetric shape in the intrinsic state before parity projection (Fig. 4). As explained in Table II, the wave function is equivalent to the $[ud]^0$-$[ud]^0\bar{s}$ cluster wave function in the Brink model [30] with $L = 1$ relative motion. After the parity projection, the $\bar{s}$ is exchanged between two diquarks. In contrast to the spatially developed cluster structure in the even-parity state, the odd-parity states $J^\pi = 1/2^-, 3/2^-$ are almost the spatially symmetric $(0s)^5$ states with spherical shapes.

As mentioned, the degeneracy of the even-parity states and the odd-parity states originates in the balance of the $L = 1$ excitation energy and the energy gain of the color-magnetic interaction. Here we consider the $L = 1$ excitation energy $\Delta E(L = 1)$ as the total energy loss in the kinetic, string, and Coulomb terms. It is important that $\Delta E(L = 1) \sim 0.3$ GeV in the pentaquark is much smaller than $\Delta E(L = 1) \sim 0.5$ GeV in the nucleon system. The reason for the relatively small $\Delta E(L = 1)$ in the pentaquark can be easily understood by the ud-uds cluster structure. In the two-body cluster state with the $L = 1$ relative motion, the $\Delta E(L = 1)$ is roughly estimated by the reduced mass $\mu = A_1A_2/(A_1 + A_2)$ of two clusters, as is given as $\Delta E(L = 1) \propto \frac{1}{\mu}$ (A_1 and A_2 are the masses of the clusters). In the nucleon, $\mu = \frac{2}{3}m_q$ is obtained from the ud-u cluster structure in the $J^\pi = 1/2^-(L = 1)$ state, whereas $\mu \sim \frac{6}{5}m_q$ for the pentaquark system is found in the ud-uds clustering. The reduced mass in the pentaquark is 9/5 times larger than that in the nucleon system, therefore, $\Delta E(L = 1)$ should be smaller in the pentaquark than in the nucleon by the factor 5/9. This factor is consistent with the present $\Delta E(L = 1)$ values.

We give a comment on the LS splitting between $J^\pi = 1/2^+$ and $3/2^+(S = 1/2, L = 1)$. In the present calculation, where the spin-obit force is omitted, the $J^\pi = 1/2^+$ and $3/2^+$ states exactly degenerate. Even if we introduce the spin-orbit force into the Hamiltonian, the LS splitting should not be large in this diquark structure because the effect of the spin-orbit force from the spin-zero diquarks is very weak as discussed in Ref. [33].

We remark that the $[ud]^0$-$[ud]^0\bar{s}$ cluster structure in the present result is different from the diquark-triquark structure proposed by Karliner and Lipkin [16] because the $ud\bar{s}$ triquark in Ref. [16] is the $(us)_6^{S=1}\bar{s}$ with the color-symmetric spin-one ud diquark. In the $(us)_6^{S=1}\bar{s}$ triquark, the $\bar{s}$ quark should be tightly bound in the triquark because of the strong color-magnetic interaction between $(us)_6^{S=1}$ and $\bar{s}$. Conversely, in the present $[ud]^0\bar{s}$ cluster, the $\bar{s}$ feels no strong color-magnetic interaction and is bound more weakly than in the $(us)_6^{S=1}\bar{s}$ triquark. The color-6 flux tubes are not taken into account in the present framework because they are excited. However, the $(us)_6^{S=1}\bar{s}$ triquark might be possible if the short-range correlation in the triquark make the flux tube short enough to be excited into the color-6 flux tube.

B. Width for KN decays

In the $\Theta^+ \to KN$ decays, it is important that the allowed decay mode in the $\Theta_1^+(J^\pi = 3/2^-)$ is D wave, which should make the Θ_1^+ state narrower than the $\Theta_0^+(J^\pi = 1/2^+, 3/2^+)$ because of the higher centrifugal barrier. We estimate the KN decay widths of these states by using a method of reduced width amplitudes [31,32]. This method has been applied for the study of α-decay width in the nuclear physics within bound state approximations. In this method, the decay width Γ is estimated by the penetrability $P_L(k, a)$ of the barrier and the reduced width $\gamma^2(a)$ as a function of the threshold energy E_{th}

and the channel radius a,

$$\Gamma = 2P_L(k,a)\gamma^2(a),$$
$$P_L(k,a) = \frac{ka}{j_L^2(ka)+n_L^2(ka)}, \quad (17)$$
$$\gamma^2(a) = \frac{\hbar^2}{2\mu a}S_{\rm fac}(a),$$

where μ is the reduced mass, k is the wave number $k = \sqrt{2\mu E_{\rm th}/\hbar^2}$, and $j_L(n_L)$ is the regular(irregular) spherical Bessel function. $S_{\rm fac}(a)$ is the probability of a decaying particle at the channel radius a. We define $\Gamma_L^0(a, E_{\rm th}) \equiv \hbar^2 k/\mu(j_L^2(ka)+n_L^2(ka))$; then, the decay width can be rewritten in a simple form as $\Gamma = \Gamma_L^0 \times S_{\rm fac}$. In the following discussion, we choose the channel radius $a = 1$ fm and $E_{\rm th} = 100$ MeV. Because the transitions between the different flux-tube configurations, a confined state $[ud][ud]\bar{s}$ and a decaying state $(udd)_1(u\bar{s})_1$, are of higher order, the $S_{\rm fac}$ should be small in general when the suppression by the flux-tube transition is taken into account. Here, we evaluate the maximum values of the widths for the $J^\pi = 1/2^+, 3/2^+$ states with the method of the reduced width amplitudes, by using meson-baryon probability considering only the simple overlap for the quark wave functions.

In case of even-parity $J^\pi = 1/2^+, 3/2^+$ states, the KN decay modes are the P wave, which gives $\Gamma_{L=1}^0 \approx 100$ MeV fm. By assuming $(0s)^2$ and $(0s)^3$ harmonic-oscillator wave functions for K^0 and p, we calculate the overlap between the obtained pentaquark wave function and the K^0p state. As explained in the previous subsection, the $J^\pi = 1/2^+, 3/2^+$ states have the ud-$ud\bar{s}$ cluster structure where five Gaussian centers are written as $\mathbf{Z}_1 = \mathbf{Z}_2 = \frac{3}{5\sqrt{2}b}\mathbf{Q}_{12}$ and $\mathbf{Z}_3 = \mathbf{Z}_4 = \mathbf{Z}_5 = -\frac{2}{5\sqrt{2}b}\mathbf{Q}_{12}$. We assume a simple K^0p wave function as follows:

$$\Phi_{K^0p} = (1+P)\mathcal{A}\left[\phi_{\mathbf{Z}_1}\phi_{\mathbf{Z}_2}\cdots\phi_{\mathbf{Z}_{N_q}}X\right], \quad (18)$$

$$\phi_{\mathbf{Z}_i} = \left(\frac{1}{\pi b^2}\right)^{3/4}\exp\left[-\frac{1}{2b^2}(\mathbf{r}-\sqrt{2}b\mathbf{Z}_i)^2 + \frac{1}{2}\mathbf{Z}_i^2\right], \quad (19)$$

where the $\mathbf{Z}$'s are chosen as $\mathbf{Z}_1 = \mathbf{Z}_2 = \mathbf{Z}_3 = a\frac{2}{5\sqrt{2}b}\mathbf{Q}_{12}/|\mathbf{Q}_{12}|$, $\mathbf{Z}_4 = \mathbf{Z}_5 = -a\frac{3}{5\sqrt{2}b}\mathbf{Q}_{12}/|\mathbf{Q}_{12}|$, and the spin-isospin-color wave function is taken to be the following:

$$X = \sum_{m_1,m_2,m_3,m_4,m_5} c_{m_1m_2m_3m_4m_5}|m_1m_2m_3m_4m_5\rangle_S \otimes |ududs\bar{}\rangle \otimes \epsilon_{abc}\delta_{ef}|abce\bar{f}\rangle_C. \quad (20)$$

The same size parameter b as that of the pentaquark is used. The coefficients $c_{m_1m_2m_3m_4m_5}$ for the spin function are taken to express the $J^\pi = 1/2^+$ proton and the pseudoscalar K^0 meson. The probability $S_{\rm fac}$ is evaluated by the overlap with the obtained $J^\pi = 1/2^+, 3/2^+$ wave function, $S_{\rm fac} = |\langle\Phi_{K^0p}|\Phi(\mathbf{Z})\rangle|^2$. [The Φ_{K^0p} and $\Phi(\mathbf{Z})$ are normalized.] The probability $S_{\rm fac} = 0.034$ fm^{-1} is evaluated by the overlap. Roughly speaking, the main factors in this meson-baryon probability are the factor $\frac{1}{3}$ from the color configuration, the factor $\frac{1}{4}$ from the intrinsic spin part, and the other factor that arises from the spatial overlap. By using the probability $S_{\rm fac} = 0.034$, the K^0p partial decay width is evaluated as $\Gamma < 3.4$ MeV. The K^+n decay width is the same as that of the K^0p decay, and the total width of the $J^\pi = 1/2^+, 3/2^+$ states is estimated to be $\Gamma < 7$ MeV. This is consistent with the discussion in Ref. [34].

It is interesting that the KN decay width of the $\Theta_1^+(J^\pi = 3/2^-)$ is strongly suppressed by the D-wave centrifugal barrier, because lower spin (S- and P-wave) decays are forbidden because of the conservation of spin and parity. Consequently, $\Gamma_{L=2}^0$ is $\approx$30 MeV fm, which is much smaller than that for the P-wave case. Moreover, the $\Theta_1^+(J^\pi = 3/2^-)$ is the state with $S^\pi = 3/2^-$ and $L = 0$, which has no overlap with the KN ($S^\pi = 1/2^-$ and $L = 2$) states in the present calculation because the spin-orbit or tensor forces are omitted. If we introduce the spin-orbit or tensor forces, the D state ($S^\pi = 1/2^-$ and $L = 2$) will be slightly mixed into the $\Theta_1^+(J^\pi = 3/2^-)$. However, the mixing component should be small because of the dominant central force in the potential. In other words, the KN probability ($S_{\rm fac}$) in the $\Theta_1^+(J^\pi = 3/2^-)$ state is expected to be more suppressed than that in the $\Theta_0^+(J^\pi = 1/2^+, 3/2^+)$ states. Considering the suppression effects in both terms Γ^0 and $S_{\rm fac}$, the $J^\pi = 3/2^-$ state should be extremely narrow. If we assume the $S_{\rm fac}$ in the $J^\pi = 3/2^-$ to be half of that in the $J^\pi = 1/2^+, 3/2^+$ states, the KN decay width is estimated to be $\Gamma < 1$ MeV.

Contrary to the narrow width of the $J^\pi = 3/2^-$ state, the $J^\pi = 1/2^-$ state should be much broader than other states because S-wave ($L = 0$) decay is allowed and therefore the centrifugal barrier is absent. We cannot evaluate the width of the $J^\pi = 1/2^-$ states with the present method, because the method of the reduced width amplitudes works only when there exist barriers in the decaying channels. If we adopt the theoretical width $\Gamma = 1.1$ GeV for the $J^\pi = 1/2^-$ states in [34] and the suppression factor $\epsilon^2 \lesssim 1/10$ because of the string transition, the width is evaluated to be $\Gamma \sim 100$ MeV, which is still too large to describe that of the observed Θ^+. We consider that the $J^\pi = 1/2^-$ states may melt away because of the coupling with KN continuum states with no centrifugal barrier.

Also in other spin-parity states, the coupling with the KN continuum states is important for more quantitative discussions on the widths. We should point out that, in introducing the meson-baryon coupling, one should not treat only the quark degrees of freedom but take into account the suppression because of the rearrangement of flux-tube topologies between the meson-baryon states and the confined states.

V. SUMMARY

We proposed a quark model in the framework of the AMD method and applied it to the $uudd\bar{s}$ system. The level structure of the $uudd\bar{s}$ system and the properties of the low-lying states were studied within the model space of the $[qq][qq]\bar{q}$ configuration, where all the (anti-)quarks are connected by the color-3 flux tubes. We predicted that the narrow $J^\pi = \{1/2^+, 3/2^+\}$ (Θ_0) and $J^\pi = 3/2^-$ (Θ_1) states nearly degenerate with the $J^\pi = 1/2^-$ states. The widths of the $J^\pi = \{1/2^+, 3/2^+\}$ states and the $3/2^-$ state are estimated

to be $\Gamma < 7$ MeV and $\Gamma < 1$ MeV, respectively. Conversely, the $J^\pi = 1/2^-$ states should be broad, and we consider that they may melt away because of the coupling with KN continuum states with no centrifugal barrier. Two spin-zero diquarks are found in the $\{1/2^+, 3/2^+\}$ states, which confirms the Jaffe-Wilczek picture. We comment that the formation of two spin-zero diquarks does not always occur in $J^\pi = \{1/2^+, 3/2^+\}$ pentaquarks. For example, in case of the $ddss\bar{u}$ system, the diquark structure disappears. Instead, a dss-$d\bar{u}$ clustering appears in the $J^\pi = \{1/2^+, 3/2^+\}$ $[ds][ds]\bar{u}$ states because the color-magnetic interaction is weaker for ds pairs than for $d\bar{u}$ pairs in OGE potential. In other words, the diquark structure is formed in such a certain pentaquark as the Θ_0^+ because of the strong color-magnetic attraction between ud quarks. The degeneracy of the $J^\pi = 1/2^-, 3/2^-, 1/2^+$, and $3/2^+$ states is realized by the balance of the kinetic and string energies and the color-magnetic interaction. The origin of the novel level structure is due to the color structure in the confined five quark system bound by the connected flux tubes.

The $J^\pi = \{1/2^+, 3/2^+\}$ ($\Theta^+_{I=0}$) states in the present results may be assigned to the experimentally observed Θ^+, whereas $J^\pi = 3/2^-(\Theta_{I=1})$ is not observed yet. One should pay attention to the properties of these states, because the production rates depend on their spin, parity, and widths. The existence of many narrow states, $J^\pi = 1/2^+, 3/2^+$, and $3/2^-$, for the Θ_0^+ and Θ_1^+ may help to explain the inconsistent mass positions of the Θ^+ among the different experiments. Especially, the double peaks of the $J^\pi = 1/2^+$ and $3/2^+$ states in the Θ_0^+ are expected. In the Θ_0^+ peaks observed in the invariant mass or missing mass spectra, it is difficult to find the possible double peaks because the statistics and the resolutions are not enough [1–9]. The analysis of the NK scattering [35] provided the upper limit $\Gamma < 1$ MeV for the widths of each peaks. Considering the suppression factor because of the gluon transitions, the possibility of the double peaks ($J^\pi = 1/2^+$ and $3/2^+$) suggested in the present works has not been excluded yet. We should comment that another explanation for the inconsistency of the experimental mass positions was suggested in Ref. [36], where a systematic lowering in mass of K^0p peaks relative to the K^+n was noted. In the $I = 1$ channel, there is no significant Θ^{++} signal in the experimental data of the invariant K^+p mass in the photo-induced reactions [5,9,37]. It is important that the widths of the $J^\pi = 3/2^-$ $\Theta_{I=1}$ should be about one order smaller than those of the $J^\pi = 1/2^+$ and $3/2^+$ for the Θ_0^+. For the Θ^{++} search, it would be helpful to choose proper entrance and decay channels based on the further investigation of the production mechanism. To compare the present findings with the experimental data in more detail, further experimental data with high resolution and high statistics are required.

Finally, we remind the reader that the absolute masses of the pentaquark in the present work are not predictions. We have an ambiguity of the zero-point energy of the string potential, which depends on the flux-tube topology in each of the meson, three-quark baryon, and pentaquark systems. In the present calculation of the pentaquark, we phenomenologically adjust it to reproduce the observed mass of the Θ^+. To predict absolute masses of unknown multiquarks with new flux-tube topologies, it is desirable to determine the zero-point energy more theoretically.

ACKNOWLEDGMENTS

The authors thank T. Kunihiro, Y. Akaishi, and H. En'yo for valuable discussions. This work was supported by the Japan Society for the Promotion of Science and Grants-in-Aid for Scientific Research of the Japan Ministry of Education, Science Sports, Culture, and Technology.

[1] T. Nakano *et al.* (LEPS Collaboration), Phys. Rev. Lett. **91**, 012002 (2003).
[2] V. V. Barmin *et al.* (DIANA Collaboration), Phys. At. Nucl. **66**, 1715 (2003).
[3] S. Stepanyan *et al.* (CLAS Collaboration), Phys. Rev. Lett. **91**, 252001 (2003).
[4] V. Kubarovsky *et al.* (CLAS Collaboration), Phys. Rev. Lett. **92**, 032001 (2004).
[5] J. Barth *et al.* (SAPHIR Collaboration), Phys. Lett. **B572**, 127 (2003).
[6] A. E. Asratyan, A. G. Dolgolenko, and M. A. Kubantsev, Phys. Atom. Nucl. **67**, 682 (2004).
[7] A. Airapetian *et al.* (HERMES Collaboration), Phys. Lett. **B585**, 213 (2004).
[8] A. Aleev *et al.* (SVD Collaboration), hep-ex/0401024.
[9] ZEUS Collaboration and S. V. Chekanov, hep-ex/0404007.
[10] J. Z. Bai *et al.* (BES Collaboration), Phys. Rev. D **70**, 012004 (2004); hep-ex/0402012.
[11] K. T. Knöpfle *et al.* (HERA-B Collaboration), hep-ex/0403020.
[12] C. Pinkenburg *et al.* (PHENIX Collaboration), J. Phys. G **30**, S1201 (2004).
[13] D. Diakonov, V. Petrov, and M. V. Polyakov, Z. Phys. A **359**, 305 (1997).
[14] R. Jaffe and F. Wilczek, Phys. Rev. Lett. **91**, 232003 (2003).
[15] S. Capstick, P. R. Page, and W. Roberts, Phys. Lett. **B570**, 185 (2003).
[16] M. Karliner and H. J. Lipkin, Phys. Lett. **B575**, 249 (2003).
[17] A. Hosaka, Phys. Lett. **B571**, 55 (2003).
[18] J. Sugiyama, T. Doi, and M. Oka, Phys. Lett. **B581**, 167 (2004).
[19] S. Sasaki, Phys. Rev. Lett. **93**, 152001 (2004); hep-lat/0310014.
[20] F. Csikor, Z. Fodor, S. D. Katz, and T. G. Kovacs, J. High Energy Phys. **0311**, 070 (2003).
[21] B. K. Jennings and K. Maltman, Phys. Rev. D **69**, 094020 (2004).
[22] Y. Kanada-En'yo, H. Horiuchi, and A. Ono, Phys. Rev. C **52**, 628 (1995); Y. Kanada-En'yo and H. Horiuchi, *ibid.* **52**, 647 (1995).
[23] Y. Kanada-En'yo, M. Kimura, and H. Horiuchi, Comptes Rendus Physique **4**, 497 (2003).
[24] J. Carlson, J. B. Kogut, and V. R. Pandharipande, Phys. Rev. D **27**, 233 (1983); **28**, 2807 (1983).

[25] O. Morimatsu, Nucl. Phys. **A505**, 655 (1989); C. Alexandrou, T. Karapiperis, and O. Morimatsu, *ibid*. **A518**, 723 (1990).
[26] J. Carlson and V. R. Pandharipande, Phys. Rev. D **43**, 1652 (1991).
[27] T. T. Takahashi, H. Matsufuru, Y. Nemoto, and H. Suganuma, Phys. Rev. Lett. **86**, 18–21 (2001); T. T. Takahashi, H. Suganuma, Y. Nemoto, and H. Matsufuru, Phys. Rev. D **65**, 114509 (2002).
[28] J. Kogut and L. Susskind, Phys. Rev. D **11**, 395 (1975).
[29] F. Okiharu, H. Suganuma, and T. T. Takahashi, hep-lat/0407001.
[30] D. Brink, *Proceedings of the International School of Physics "Enrico Fermi,"* course 36, Varenna 1966, edited by C. Bloch (Academic Press, New York, 1966), p. 247.
[31] H. Horiuchi and K. Ikeda, *Cluster Model of the Nucleus, International Review of Nuclear Physics*, edited by T. T. S. Kuo and E. Osnes (World Scientific, Singapore, 1985), Vol. 4, p. 1.
[32] H. Horiuchi and Y. Suzuki, Prog. Theor. Phys. **49**, 1974 (1973), and references therein.
[33] By J. J. Dudek and F. E. Close, Phys. Lett. **B583**, 278 (2004).
[34] C. E. Carlson *et al*., Phys. Rev. D **70**, 037501 (2004); hep-ph/0312325.
[35] R. N. Cahn and G. H. Trilling, Phys. Rev. D **69**, 011501(R) (2004).
[36] Q. Zhao and F. Close, hep-ph/0404075.
[37] H. G. Juengst (CLAS Collaboration), nucl-ex/0312019.